ORIGINAL PAPER

Monitoring the dynamic behaviour of soil loss using geospatial techniques in the Kosi river basin

Aadil Towheed[1] · Thendiyath Roshni[1] (ORCID)

Abstract

Due to frequent floods and subsequent high sediment yield in the Kosi river basin, it is imperative to evaluate the dynamic behaviour of soil erosion intensity. In the present study, the effects of percentage slope of the terrain, crop management factor and average annual rainfall on soil erosion intensity for the years 2009 and 2019 have been studied. The rainfall data for seven rain gauge stations have been collected from India Meteorological Department (IMD) Pune for the period 1985–2017. The soil erosion intensity for the years 2009 and 2019 have been estimated using Revised Universal Soil Loss Equation (RUSLE), and the results are grouped under slight erosion, mild erosion, moderate erosion, intensive erosion and severe erosion intensities. It was found that the percentage area of soil erosion decreases from 52.46 to 45.39% for slight erosion intensity slice and increases for all other soil erosion intensity slices. Change intensity (CI) of soil erosion from 2009 to 2019 has been evaluated, and the results reveal that 66.45% area comes under the stable zone. The relations have been established among parameters used in RUSLE and found that soil erosion increases with the increase in crop management factor (C) up to 0.5 for 2009 and 0.8 for 2019 and then the value decreases in both the years. It was also noticed that the soil erosion increases with the percentage slope of the terrain up to one degree and then drastically decreases. The relationship between average annual rainfall and soil erosion intensity has also been established and analysed. The results of the present study provide a significant implication to water resource experts for the planning of soil conservation measures in the Kosi river basin.

Keywords RUSLE · Kosi river · Dynamic monitoring · Change intensity · Soil erosion intensity · Crop management factor

Introduction

Soil erosion is broadly granted as a menace to the ecosystem, sustainable agriculture and fertility of land. The loss of nutrients in the top soil leads to a worldwide threat to socio-economic conditions (Naipal et al. 2015; Robinson et al. 2017). Also, soil erosion has been one of the most serious issues in the environment of human altered mountains (Vijith et al. 2012). A report by Boardman (2006) has highlighted the decrease in soil health and its quality on global basis. In India, around 175 Mha of area undergoes intense

soil erosion process out of its total 328 Mha area (Narayana 1984). According to the estimates of National Bureau of Soil Survey and Land Use Planning (NBSS & LUP) in India, around 146.8 Mha (45%) of the total geographical area of the country (328 Mha) is very much prone to soil erosion and gets aggravated due to surface runoff (Bhattacharyya et al. 2015). The most important cause of degradation problem in India is water erosion which takes part in the rill erosion as well as the deformation of terrain. The average soil loss of India was around 16.4 t ha^{-1} year^{-1} based on the existing soil loss obtained from the first approximation analysis and an annual soil loss of 5.3 billion tons all over the country (Narayana and Babu 1983). Soil erosion pulls out the fertile soil (Bhattacharyya et al. 2015), which thereby causes degradation of land and its fertility (Lal 2001).

Due to the increase in enormous deforestation, mining, cultivation on slopes and extensive construction of roads, the lower Himalayan region is in a deteriorating condition. Construction work as well as deforestation is the example which causes exacerbation in soil erosion and the transportation

✉ Thendiyath Roshni
  roshni@nitp.ac.in

  Aadil Towheed
  aadil.ce17@nitp.ac.in

[1] Department of Civil Engineering, National Institute of Technology Patna, Patna, Bihar 800005, India
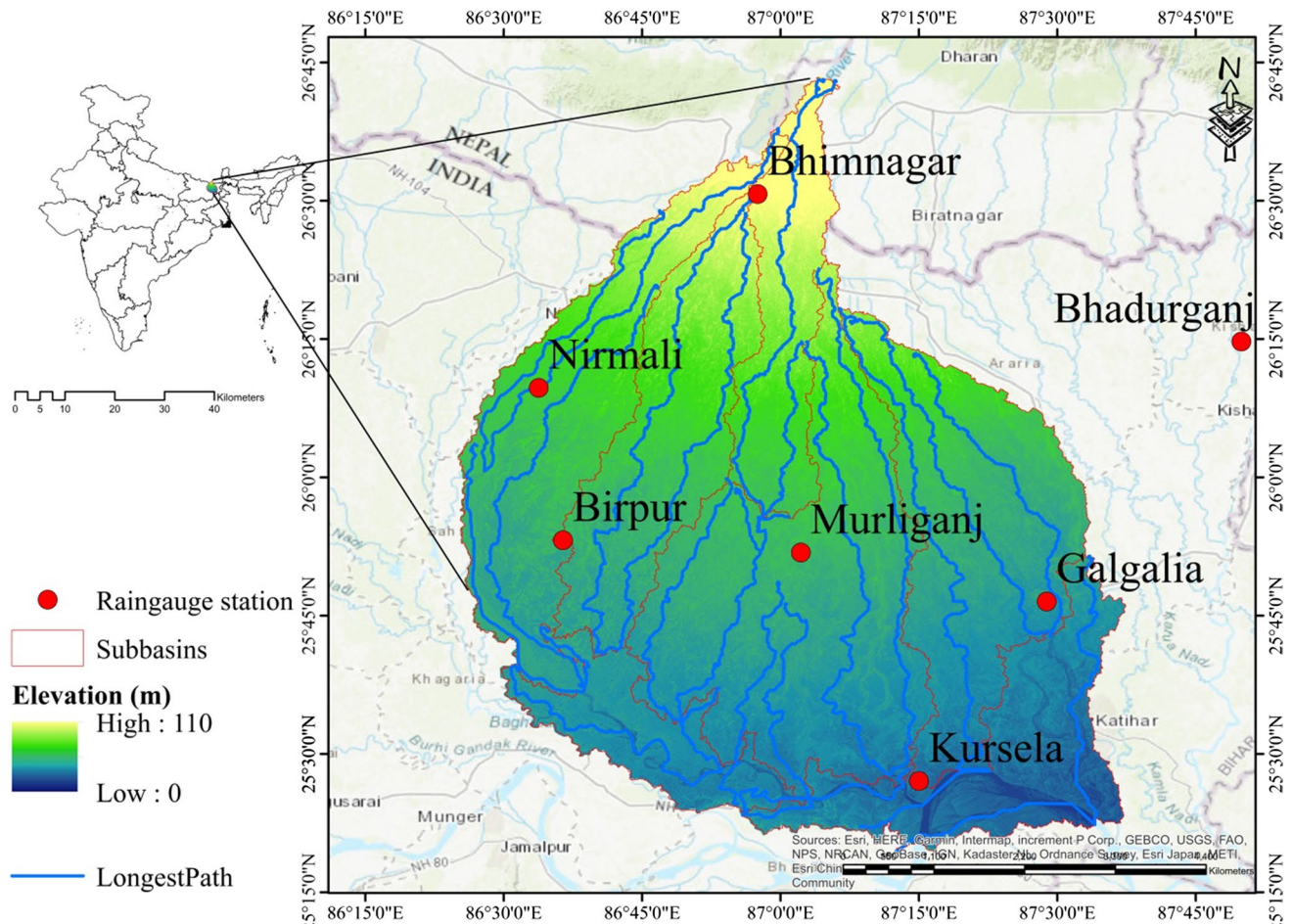
Fig. 1 DEM of the Kosi river basin in India and location of the 7 rain gauge stations

of sediments and thereby degradation of land and flooding impact (Bathrellos et al. 2017). Nearly, an area of 3 Mha in the north eastern Himalaya is severely eroded due to "Shifting Cultivation" (Narayana 1987). Singh and Gupta (1982) estimated annual soil loss through the Himalayan hills as 28.2 t ha^{-1} year^{-1}. The Kosi river originates in the high mountains of China and Nepal, and it joins Bay of Bengal through the alluvial plains of north Bihar in India (Sinha et al. 2018). The avulsion of Kosi river has resulted into a plenty of paleochannels around its megafan, and they convey the transfer of flux on the surface and may affect the topography of the megafan (Kumar et al. 2014). The Kosi basin has a typical characteristics of high and severe erosion and leads to enormous sedimentation and thereby affect the storage infrastructure (filling of dammed lakes) and agricultural land and results in fluvial hazards in the downstream (Uddin et al. 2016).

There are around 82 models including Universal Soil Loss Equation (USLE) (Wischmeier and Smith 1978), Revised Universal Soil Loss Equation (RUSLE) followed by Water Erosion Predicton Project (WEPP) (Nearing et al. 1989) and European Soil Erosion Model (EUROSEM)

(Morgan 2005) used for the estimation of soil loss. RUSLE is an empirical model and the most popular tool to evaluate hazards due to soil erosion, and it is self-deprecating to implement in the developing countries where complex models have limitations due to inadequate data inputs (Uddin et al. 2016). The RUSLE is a deterministic approach and is based on erosion in the USA-based studies despite remotely sensed data (Wischmeier and Smith 1978; Renard et al. 1997). Despite, the RUSLE model is frequently used for the evaluation of soil loss risk and can be implemented regionally and globally (Borrelli et al. 2016). RUSLE model has been used for estimation of soil loss in Bohai Rim, China (Xu et al., 2013); Guizhou Province, China (Yue-qing et al. 2008); Western Qinling Mountains, China (Zhu et al. 2021); in the mining sites of Kiruburu and Meghahatuburu, India (Kayet et al. 2018); in Ghana, West Africa (Ashiagbor et al. 2013); Kelani river basin in Sri Lanka (Fayas et al. 2019); Kirkuk Governorate, north of Iraq (Al-Abadi et al. 2016) and many more. Also, Rozos et al. (2013) utilized the RUSLE for predicting the failure of slope due to soil erosion in N. Euboea, Greece.

Fig. 2 Flowchart of the study
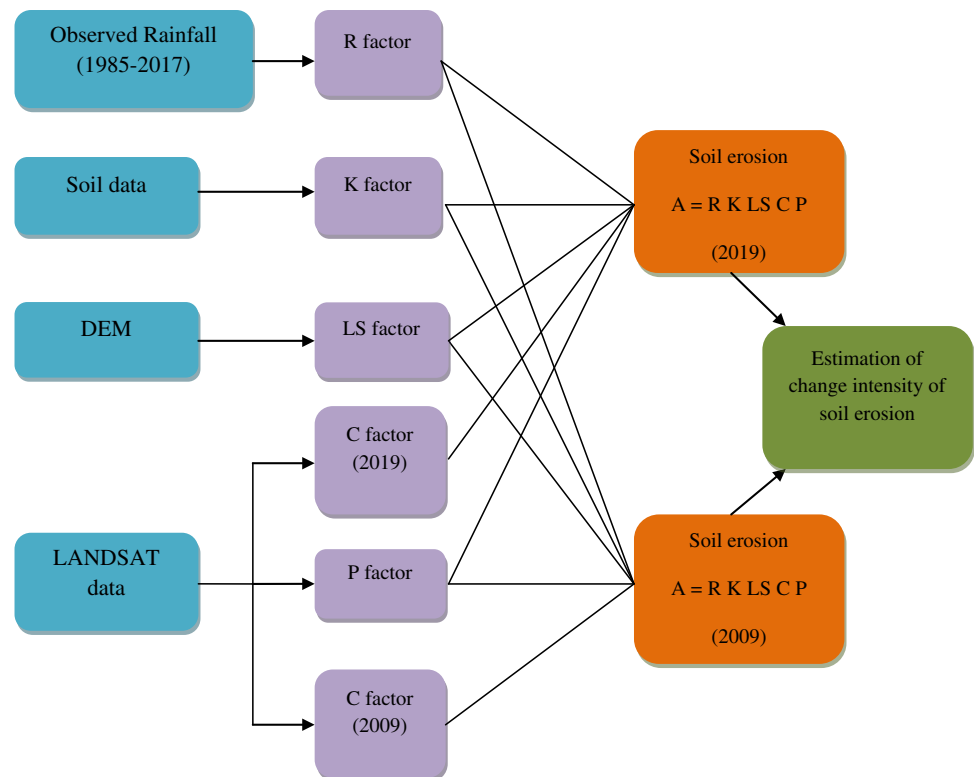
The factors included in RUSLE model have their own role to play in the estimation of soil erosion. The investigation by Jemai et al. (2021) mainly focused on the estimation of soil loss used to determine areas with a high risk of erosion, notably the spatial variability modes of the parameters controlling this phenomenon. The vegetation is one of the most important factors and the quickest responsive parameter among all parameters (Estrada-Carmona et al. 2017) that can be managed by farmers in order to control the erosion (Panagos et al. 2015). The C factor is regulated according to the vegetation density and its condition (Reusing et al. 2000). Soil erosion is one of the major issues in India in the context of rapid change in land use land cover (LULC) (Rajbanshi and Bhattacharya 2020) as well as slope of the terrain (Li et al. 2017). Due to the accelerated and intense erosion of Kosi river basin, various studies (Ganasri and Ramesh 2016; Uddin et al. 2016) have focused only on the severity and prioritize the soil erosion level, but no researches are well documented on the effects of slope of the terrain, land use and rainfall. High sediment flux in the Kosi river basin during the rainfall and restricted space within the channel reinforces the siltation and subsequently leads to floods (Mishra and Sinha 2020). In the study of Towheed and Roshni (2021), the authors have checked for the impact of climate change on soil erosion under different general circulation models (GCMs) and their corresponding scenarios. However, effects of each parameter have not been studied in the past and present time period. Zhu et al. (2021) used

RUSLE model and with the help of GIS assessed soil erosion in the Maiji district to analyse the dynamic behaviour in the years 2000, 2005, 2010 and 2015. It is compulsive to estimate and monitor the dynamic behaviour of the soil loss considering the vegetative cover and topography of the Kosi river basin which is one of the largest basins of India. The results of the study worldwide revealed that the spatiotemporal variation of soil loss is site specific, and the estimations of soil loss associated with land use and topography have not been studied so far. Hence, the objectives of this study are (i) to estimate the change intensity of annual soil loss between years 2009 and 2019 and (ii) to analyse the variation of annual soil loss with cover management factor (C), percentage slope of the terrain and average annual rainfall. This paper yields a better understanding of soil loss dynamics due to the various parameters in the Kosi river basin, lying in the lower Himalayan regions using remote sensing images and RUSLE model.

Study area and data description

The Kosi river is one of the major tributaries of the Ganga river. This river is known as the "Sorrow of Bihar" as it causes frequent floods in Bihar. The main cause behind the selection of Kosi basin is that it has been a substantial issue of rapid bank erosion and sediment yield due to which shifting of channels taking place within the basin (Mishra and
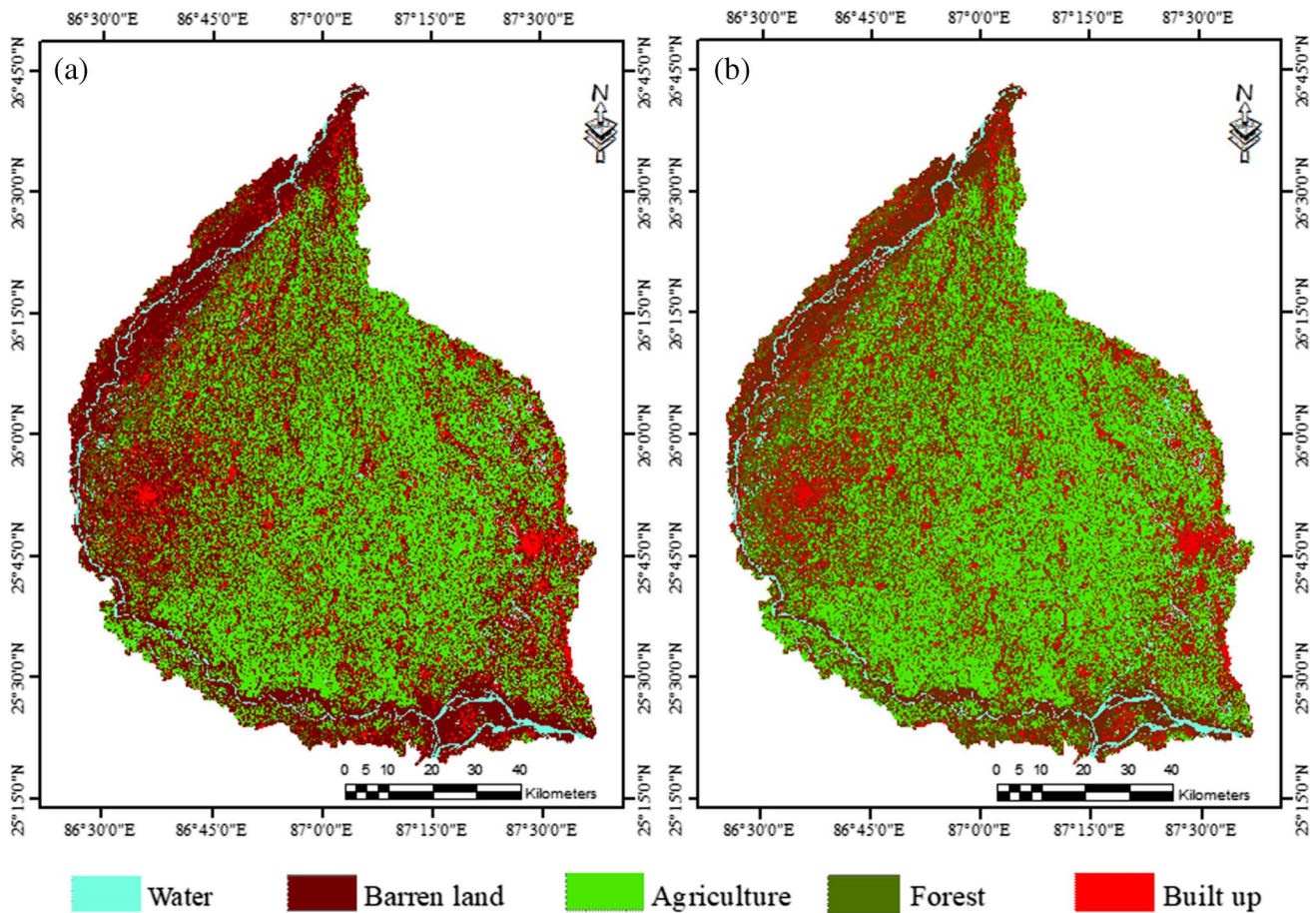
Fig. 3 Land use maps for the years **a** 2009 and **b** 2019

Sinha 2020). Kosi river flows in the North Bihar plain and covers an area of around 11,410 km². The Kosi river basin is located between latitude 25° 19′ 18″ N – 26° 43′ 30″ N and longitude 86° 20′ 0″ E and 87° 40′ 00″ E. It originates from the Himalayan region in Nepal and occupies a large area in Tibet and Nepal. The river enters Bihar (India) region near Bhimnagar and joins the Ganga river near Kursela, Katihar district, Bihar. The major tributaries of Kosi river are Bagmati, Bhutibalan, Kamlabalan, etc. Ten districts of Bihar are covered in this drainage basin (Towheed and Roshni 2021).

The daily rainfall data for a period of 33 years, i.e. from 1985 to 2017, were obtained from India Meteorological Department (IMD) Pune for 7 available rain gauge stations (Bhimnagar, Nirmali, Bhadurganj, Birpur, Murliganj, Galgalia and Kursela) and shown in Fig. 1. The SRTM 1 Arc-Second (Shuttle Radar Topography Mission)-based digital elevation model (DEM) having 30 m resolution for the year

Table 1 Assigned values of *P* factor (Yang et al. 2003) for different LULC types

LULC types	Agriculture	Water	Barren land	Built up	Forest
P factor	0.5	1	1	1	1

2019 was obtained from the earth explorer (https://earthexplorer.usgs.gov/). The land use maps were extracted using Landsat 8 (Al-Abadi et al. 2016) in 2019 and Landsat 4–5 in 2009 also obtained from the USGS (Anjali and Roshni 2021).

Methodology

In this study, annual soil erosion has been estimated for the 2 years (2009 and 2019), keeping crop management (C) factor as a variable in the RUSLE. Variations of the annual soil erosion and other parameters like C factors, topography of the study area and average annual rainfall in both the years in Kosi river basin have also been analysed. The detailed methodology of this study is shown in the flowchart given in Fig. 2.

Changes in annual soil erosion from 2009 to 2019

The soil loss is estimated using RUSLE, which is proposed by Wischmeier and Smith (1978) and is shown in Eq. 1.

$$A = R \times K \times LS \times C \times P \tag{1}$$

where A represents the annual soil loss per unit area (t ha^{-1} year^{-1}), R is the rainfall-runoff erosivity factor (MJ mm ha^{-1} h^{-1} year^{-1}), K is the soil erodibility factor (t ha h ha^{-1} MJ^{-1} mm^{-1}), LS is the length and slope factor, C is the crop management factor, and P is the support practice factor (Renard et al. 1997).

Rainfall-runoff erosivity (R) factor

Rainfall-runoff erosivity factor is defined as the ability of rainfall drops to erode soil particle from its original place and contributes to the runoff. Xu et al. (2008) concluded that the rainfall runoff erosivity is associated with the amount of runoff resulted from rainfall events. R factor is calculated using the formula given by Renard and Freimund (1994):

$$R = 0.04830 \, P^{1.610} (\text{when} \, P < 850\text{mm}) \tag{2}$$

$$R = 587.8 - 1.219P + 0.004105P^2 (\text{when} \, P > 850\text{mm}) \tag{3}$$

where P is average annual rainfall in mm.

Soil erodibility (K) factor

Soil erodibility factor is mainly dependent on the type of soil within the study area. The amount and frequency of runoff produced by specific rainfall input is measured for a standard condition, which is defined for a 22.6-m-long unit plot and gradient of 9% maintained in uncultivated land (Kim 2006). The K factor is calculated using formula (Yang et al. 2003):

$$K = \frac{1}{7.6}\left\{0.2 + 0.3exp\left[-0.0256\left(1 - \frac{SIL}{100}\right)\right]\right\}\left(\frac{SIL}{CLA + SIL}\right)^{0.3}\left(1 - \frac{0.25OM}{Org + exp(3.72 - 2.95OM)}\right)\left(1 - \frac{0.75SN}{SN + exp(-5.51 + 22.9SN)}\right) \tag{4}$$

where SN is given as $SN = (1 - SAN)/100$ and CLA, SIL, SAN and OM are represented as percentage content of clay, silt, sand and organic matter respectively. The value of K factor depends on the soil type (sand, silt, organic matter and clay) within the basin.

Length and slope (LS) factor

Length and slope factor was evaluated using Shuttle Radar Topography Mission (SRTM 1 Arc-Second) having resolution of 30 m obtained from United States Geological Survey (USGS)-based earth explorer (https://earthexplorer.usgs.gov/) (Kumar et al. 2020). LS factor is calculated using Eq. 5 as follows:

$$LS = \left(\frac{Q_a M}{22.13}\right)^y * (0.065 + 0.045 * S_g + 0.0065 * S_g^2) \tag{5}$$

where S_g = Grid slope in percentage; Q_a = flow accumulation grid; M = grid size and y = dimensionless exponent which ranges from 0.2 to 0.5.

Crop management (C) factor

The C factor is estimated using Normalised Difference Vegetation Index (NDVI) from the months October to December. The NDVI is defined as the ratio of difference between reflectance in red (RED) wavelength bands and near infrared (NIR) wavelength bands to the summation of near infrared wavelength bands and red wavelength bands (Kumar and Roshni 2019). Landsat 4–5 and Landsat 8 images have been utilised for the calculation of NDVI for the years 2009 and 2019 and is shown in the equation (Eq. 6)

$$NDVI = \frac{NIR - RED}{NIR + RED} \tag{5}$$

The C factor is evaluated using Eq. 7 (Zhou et al. 2008) as follows:

$$C = exp\left[-\alpha\left(\frac{NDVI}{\beta - NDVI}\right)\right] \tag{6}$$

where the coefficient α is 2 and β is 1 which are unitless parameters. Using these parameters, the shape of the curve relating NDVI (NDVI – C curve) can be determined (Gupta and Kumar 2017).

Support practice (P) factor

Support practice factor is estimated using land use land cover map as the lands are assigned to different types of land covers (Yang et al. 2003). The LULC maps were prepared (Fig. 3) using Landsat 4–5 and Landsat 8 (Himayoun and Roshni 2020) images from October to December 2009 and 2019 and were verified with ground survey. Table 1 shows the assigned values of P factor to the land use within the study area (Yang et al. 2003).
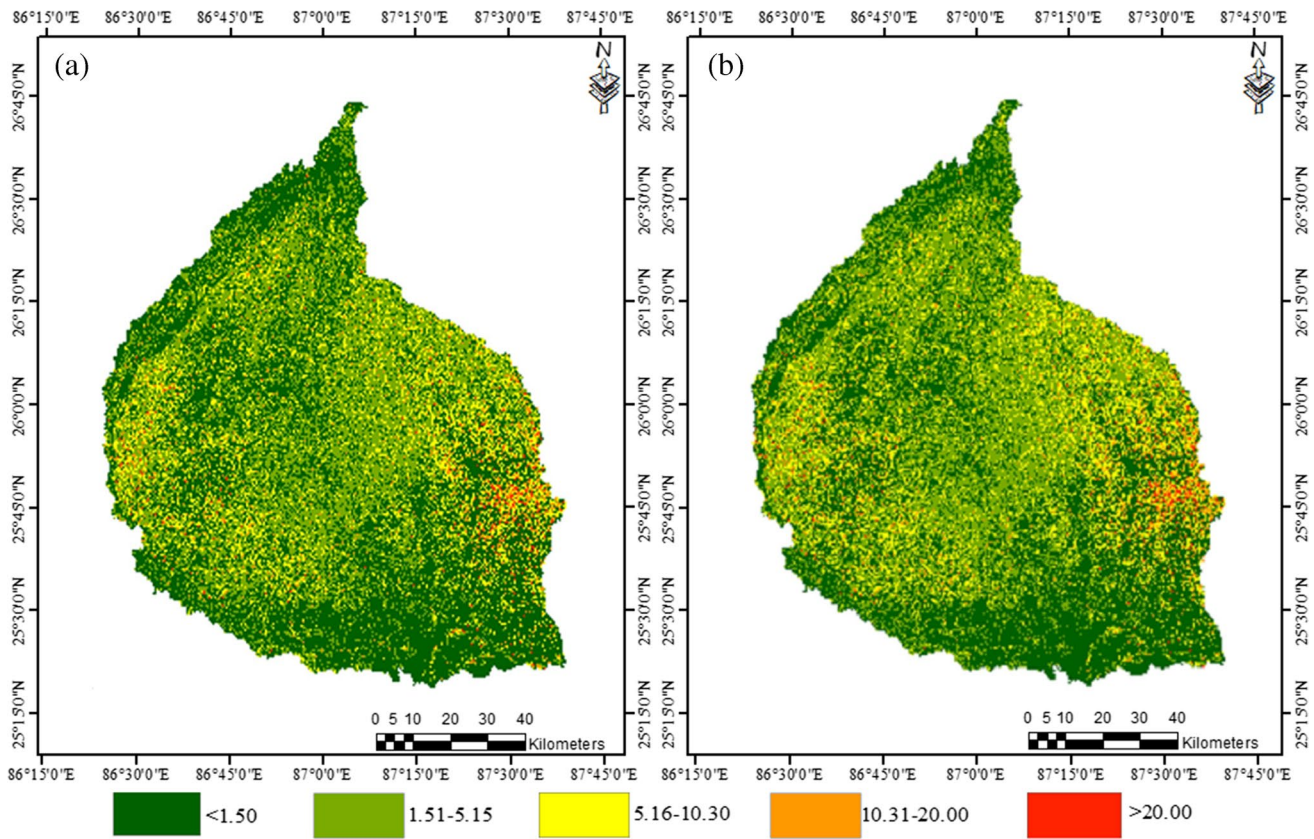
Fig. 4 Spatial variation of soil erosion (t/ha/y) based on the two different cover management factors for the years **a** 2009 and **b** 2019

Results

Spatial variation of soil loss in the year 2009 and 2019

Supervised classification has been adopted to classify the Landsat data into five classes such as Agriculture (temporary vegetation), Forest (permanent vegetation), Barren land (bare soil and fallow land), Built up and Water bodies. Temporary vegetation (agriculture class) includes grass, crops, healthy plants and shrubs and permanent vegetation includes large trees and forests, whereas built up include roads, paved areas, buildings or houses and industrial areas. Thousands of training samples have been taken to define the area to be used for training sites for each class of land cover. This is done with the help of digitizing features on screen for years 2009 and 2019 and is shown in Fig. 3. Using the C factor, the soil losses were evaluated with the help of RUSLE equation. Landsat images of months between October and December have been utilized for the calculation of C factor. Figure 4a and b show the spatial variation of soil erosion maps for the year 2009 and 2019 respectively. Soil erosion intensity (SEI) is classified into five categories as SEI < 1.5 t/ha/year is slight erosion, 1.51 t/ha/year < SEI < 5.15 is mild erosion, 5.16 t/ha/year < SEI < 10.30 t/ha/year is moderate erosion, 10.31 t/ha/year < SEI < 20.00 t/ha/year is intensive erosion, and SEI > 20.00 t/ha/year is severe erosion (Uddin et al. 2016).

Table 2 Soil erosion intensity for the years 2009 and 2019 and area of erosion in hectare

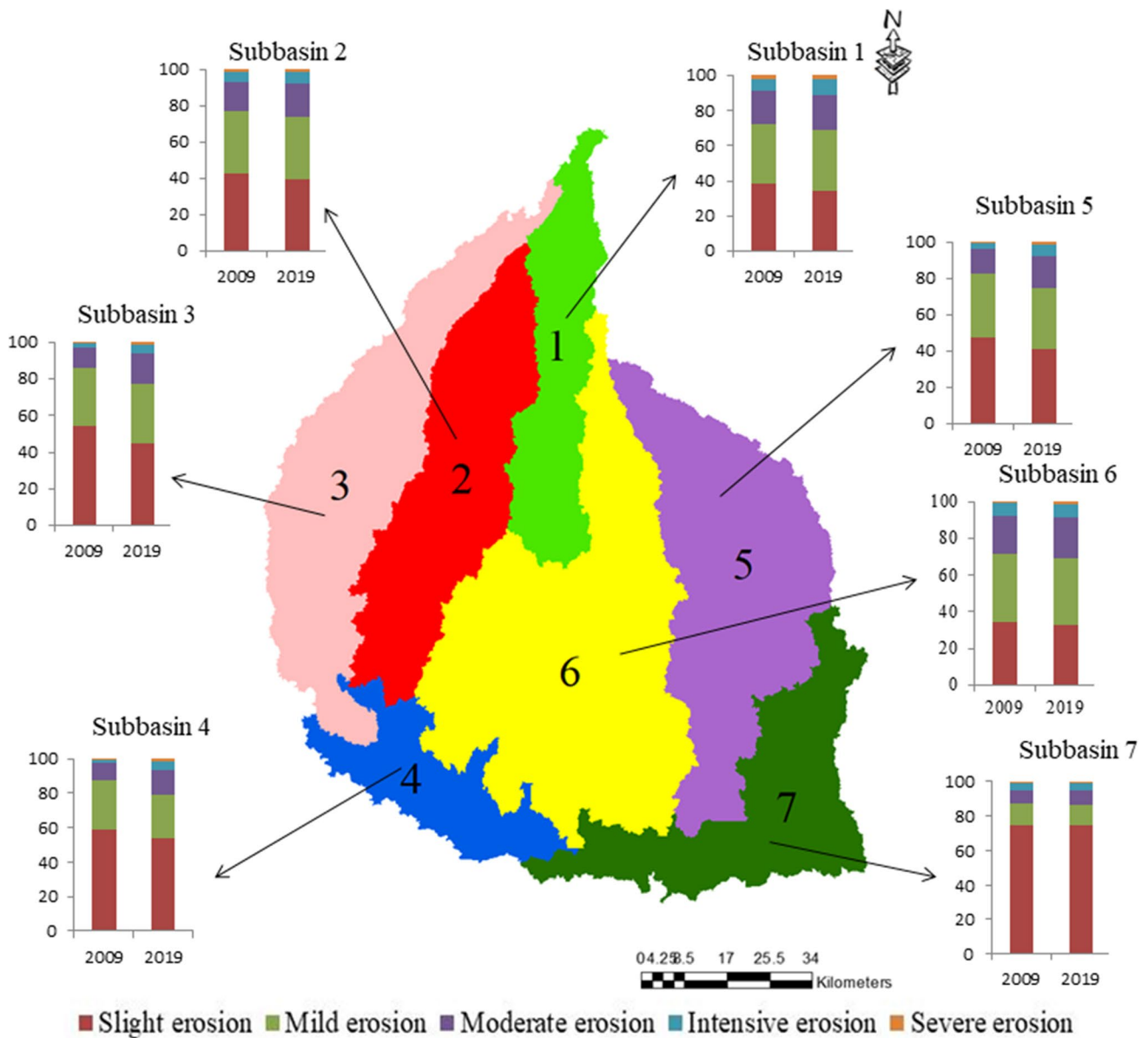| Erosion intensity	Erosion rate (t/ha/y)	2009		2019	
		Area (*100 ha)	%Area	Area (*100 ha)	%Area
Slight erosion	< 1.50	5338.94	52.46	4619.48	45.39
Mild erosion	1.51–5.15	3364.56	33.06	3402.81	33.44
Moderate erosion	5.16–10.30	1149.04	11.29	1600.31	15.73
Intensive erosion	10.31–20.00	286.62	2.82	473.89	4.66
Severe erosion	> 20.00	37.56	0.37	80.23	0.79

Fig. 5 The subbasin wise soil loss bar chart of Kosi river basin for the years 2009 and 2019

The area of soil erosion of the years 2009 and 2019 has been evaluated with the five soil erosion intensity slices mentioned above and tabulated in Table 2. The percentage of area affected in different soil erosion intensity slices has also been evaluated. The percentage area under the slight erosion intensity had reduced from 52.46 to 45.39, and a small increase in the % area of mild, moderate, intensive and severe erosion was noticed.

Percentage area of subbasin wise soil erosion in 2009 and 2019

There are seven subbasins that have been obtained after merging 27 delineated subbasins using ArcSWAT. Figure 5 shows seven subbasins labelled from one to seven with different colours. Each subbasin is tagged with the bar chart of percentage area of soil erosion with different soil erosion intensity slices

Table 3 Area of delineated seven subbasins using ArcSWAT

Subbasins	1	2	3	4	5	6	7
Area (*100 ha)	981.28	1553.41	1834.63	728.73	2027.36	2934.60	1303.86

Table 4 Percentage area of soil erosion in 7 subbasins in 2009

Erosion intensity	Erosion rate (t/ha/year)	Percentage area of erosion in subbasins						
		1	2	3	4	5	6	7
Slight erosion	< 1.50	38.03	42.79	54.54	58.89	47.92	34.32	74.91
Mild erosion	1.51–5.15	34.51	34.73	31.49	28.87	34.59	37.51	12.25
Moderate erosion	5.16–10.30	18.42	15.85	10.89	9.93	13.68	20.52	7.79
Intensive erosion	10.31–20.00	7.27	5.28	2.72	1.91	3.45	6.69	4.04
Severe erosion	> 20.00	1.77	1.35	0.36	0.40	0.36	0.96	1.01

Table 5 Percentage area of soil erosion in 7 subbasins in 2019

Erosion intensity	Erosion rate (t/ha/year)	Percentage area of erosion in subbasins						
		1	2	3	4	5	6	7
Slight erosion	< 1.50	34.45	39.51	44.72	53.76	41.20	32.52	74.63
Mild erosion	1.51–5.15	34.56	34.18	32.98	25.32	33.25	36.46	11.52
Moderate erosion	5.16–10.30	19.98	18.47	15.98	14.60	18.05	22.24	8.57
Intensive erosion	10.31–20.00	8.71	6.63	5.43	5.16	6.32	7.39	4.25
Severe erosion	> 20.00	2.30	1.21	0.89	1.16	1.18	1.39	1.03

for 2009 and 2019. The five different slices of soil erosion intensity are same as discussed in "Spatial variation of soil loss in the year 2009 and 2019". The area of each subbasin is given in Table 3 with subbasin 6 having the largest area (2934.60 * 100 ha) and subbasin 4 with the least (728.73 * 100 ha).

The percentage areas of soil erosion of seven subbasins are also tabulated in Tables 4 and 5. The results show that the highest areas of soil erosion were covered in the slice of slight erosion in 2009 and 2019 in subbasin 7 (i.e. 74.91% and 74.63%). For slight erosion intensity slice, the least percentage area of soil erosion is in subbasin 6 in both years 2009 and 2019. In all subbasins, the percentage area of slight erosion decreases in the year 2019 as compared to 2009. For mild erosion, there is decrease in the percentage area of soil erosion in all subbasins except two subbasins 1 and 3. In the moderate soil erosion slice, there is an increase in percentage soil erosion areas, and major increase is observed in subbasins 2, 3, 4 and 5 for the year 2019. For intensive soil erosion, the percentage areas of soil erosion increases in all subbasins, and a major increase was observed in subbasins 3, 4 and 5 for the year 2019. Lastly, in the severe soil erosion slice, the percentage area of soil erosion was least in all subbasins for the 2 years. The percentage area of soil erosion for the slice of severe erosion increases slightly in all subbasins except in subbasin 2. Overall, the highest percentage area of soil erosion is 74.91 in slight intensity erosion slice which occurred in subbasin 7.

CI in soil erosion during 2009 to 2019

Change intensity (CI) has been evaluated from 2009 to 2019 in order to monitor the spatiotemporal variation in the soil erosion intensity. According to the histogram and standard deviation of images obtained in ArcGIS 10.3 for

the years 2009 and 2019, CI was divided into seven levels: intensive decrease (CI < − 5.68 t/ha/year), moderate decrease (− 5.67 t/ha/year < CI < − 2.34 t/ha/year), mild decrease (− 2.33 t/ha/year < CI < − 0.80 t/ha/year), stable (− 0.79 t/ha/year < CI < − 0.74 t/ha/year), mild increase (− 0.73 t/ha/year < CI < 4.07 t/ha/year), moderate increase (4.08 t/ha/year < CI < 13.31 t/ha/year) and intensive increase (CI > 13.32 t/ha/year). Figure 6 shows that most of the area is covered under stable zone which has maximum percentage of 66.45% area followed by a mild decrease CI of 20.99% area. The intensive increase CI is found only for a small area of 0.07% and is shown in Table 6.

Based on the CI map shown in Fig. 6, it is visually analysed that all subbasins have mostly stable CI except for subbasins 3 and 5. Hence, the changes in LULC patterns of the subbasins 3 and 5 are taken into consideration, and the percentage changes in land use are plotted in Fig. 7. The results also show that the percentage of both agricultural and forest area decreases by 4%; however, water, barren land and built up portions increase by 2%, 4% and 2% respectively for subbasin 3 whereas for subbasin 5, agriculture and forest decease by 4% and 2% respectively; however, water, barren land and built up increase by 2%, 3% and 5% respectively.

Relation between cover management factor and soil erosion intensity

The change in land use types is one of the controllable factors which have remarkable relationships with the change in soil erosion intensity (Guo et al. 2012). A sample of 30,000 random points has been created in the ArcGIS 10.3 using constraining feature class as shapefile of the study area. Crop management factor for the years 2009

Fig. 6 Change Intensity in soil loss between the years 2009 to 2019 of Kosi basin
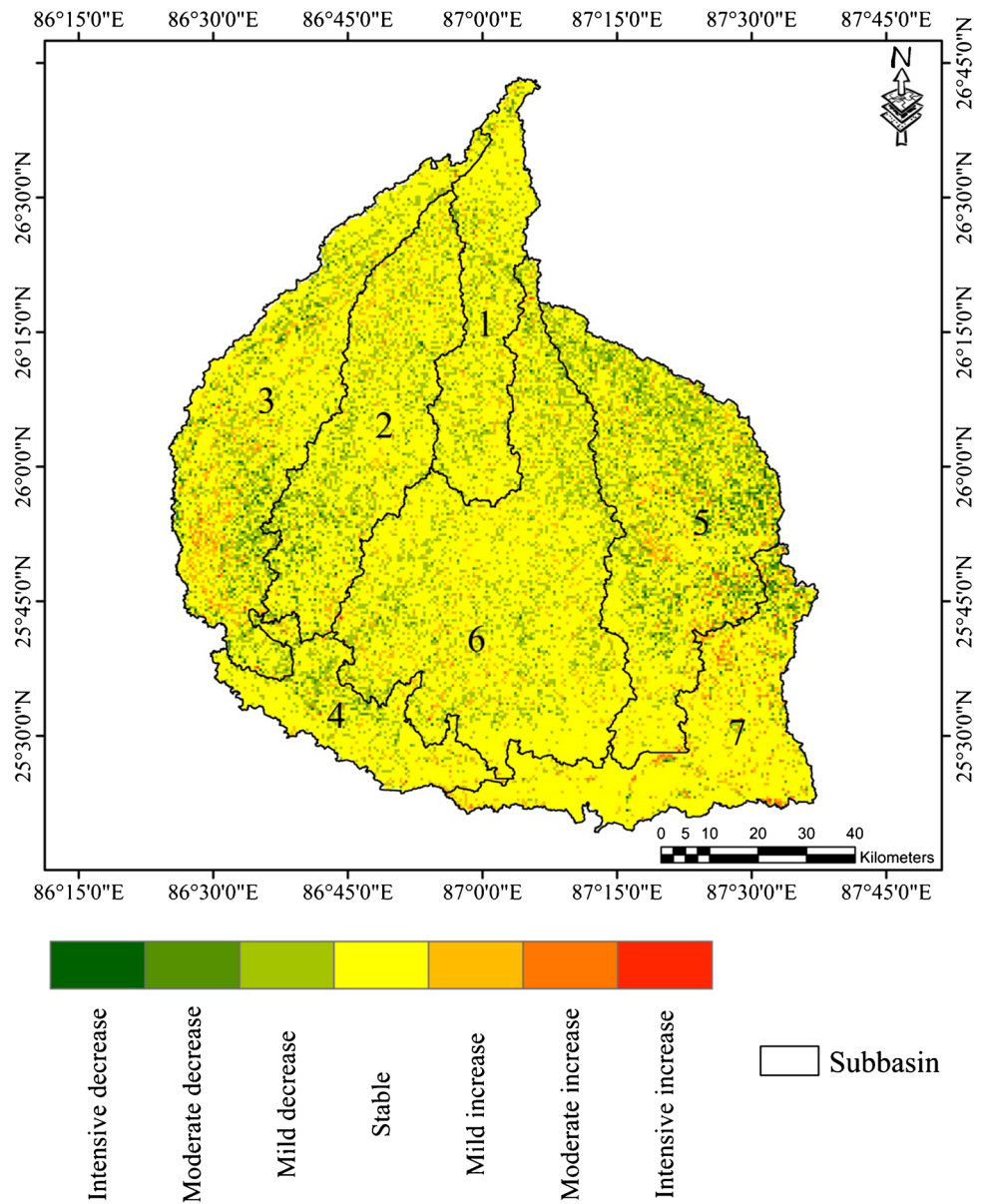
and 2019 (October-December) and corresponding soil erosion intensity have been taken as multivalues to find

Table 6 Percentage area of change intensity in soil erosion from years 2009 to 2019

Change intensity	Range (t/ha/y)	Area (sq. km)	% Area
Intensive decrease	< − 5.68	60.64	0.60
Moderate decrease	− 5.67 to − 2.34	523.56	5.14
Mild decrease	− 2.33 to − 0.80	2135.76	20.99
Stable	− 0.79 to − 0.74	6762.48	66.45
Mild increase	− 0.73 to 4.07	588.86	5.79
Moderate increase	4.08–13.31	98.18	0.96
Intensive increase	> 13.31	6.76	0.07

the relationship between them. Figure 8a and b show the scatter plots between soil erosion intensity and crop management factor in 2009 and 2019, and the patterns of the data show a bell shaped in both the years. However, the shape of the plot in 2009 is slightly skewed towards left that indicates the congestion of soil erosion intensity starts at the early stage and gets its peak. In the year of 2019, the points are concentrated for C factor ranges from 0.4 to 1.2. The patterns in Fig. 8a and b show that soil erosion intensity increases with the increase in value of *C* factor and get their peaks at 0.5 and 0.8 respectively for both the years. The random samples show the peak of soil erosion intensity is 30 t/ha/year for 2009 and 35 t/ha/year for 2019; however, the congestion of some points in 2019 is

Fig. 7 Pie chart of percentage area of LULC between sub-basins 3 and 5
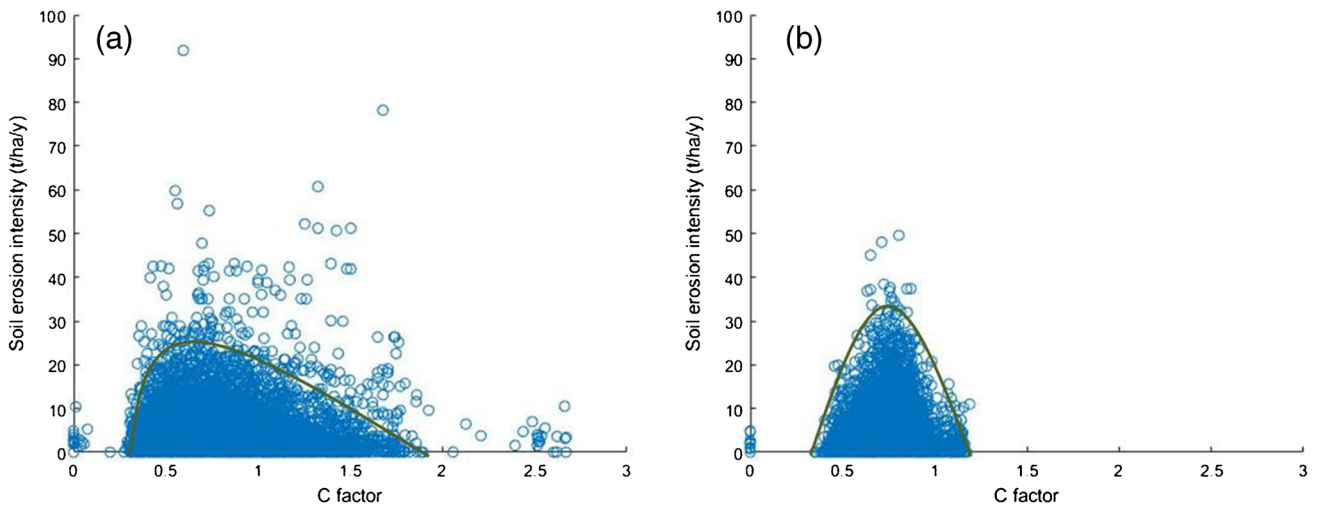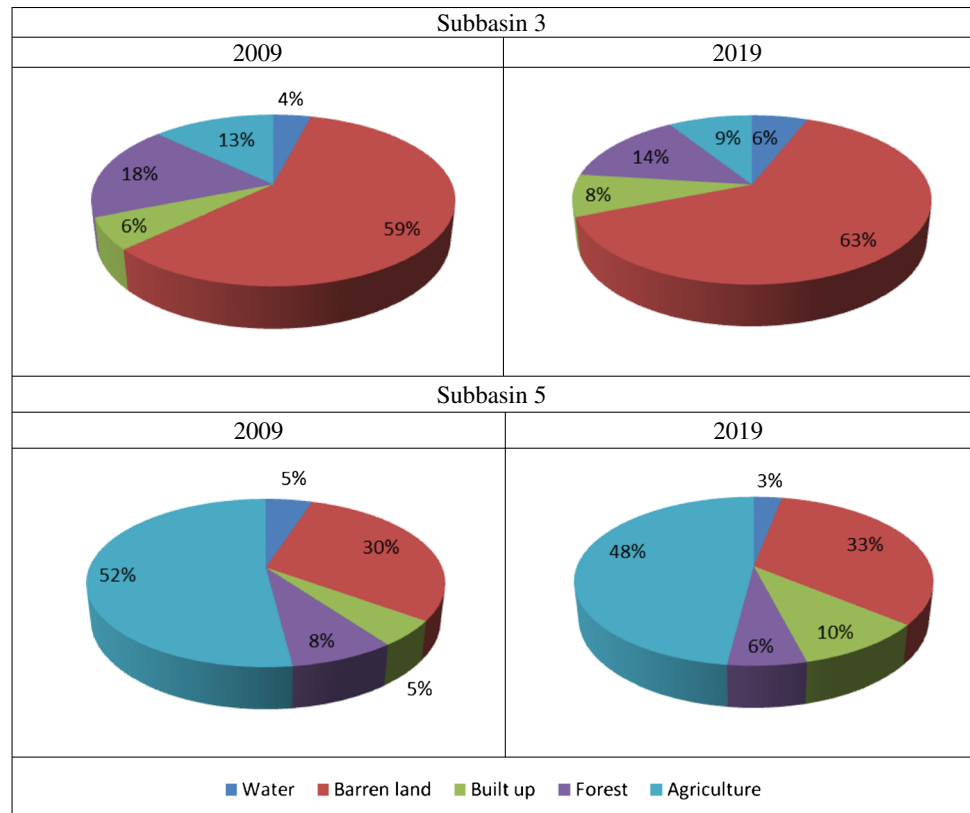

Fig. 8 Variation of soil erosion intensity (t/ha/year) with respect to *C* factor for the month October **a** 2009 and **b** 2019

beyond 35 t/ha/year. In addition, more scatter of *C* factor is observed in 2009 compared to the *C* factor in 2019.

Relation between slope of the terrain and soil erosion intensity

The slope of the terrain has an important role for influencing the spatial pattern of soil erosion intensity (Guo et al.

2012). In order to investigate the relationship between soil erosion intensity and slope of the terrain of the Kosi river basin, the same number of random points has been used, and the results have been plotted in Fig. 9. It is interesting to note that even at zero-degree slope, significant soil erosion is visible. It is also observed that the peak of the soil erosion intensity of 60 tha^{-1} year^{-1} lies in the range of 0–1 degrees and then it decreases with the slope.
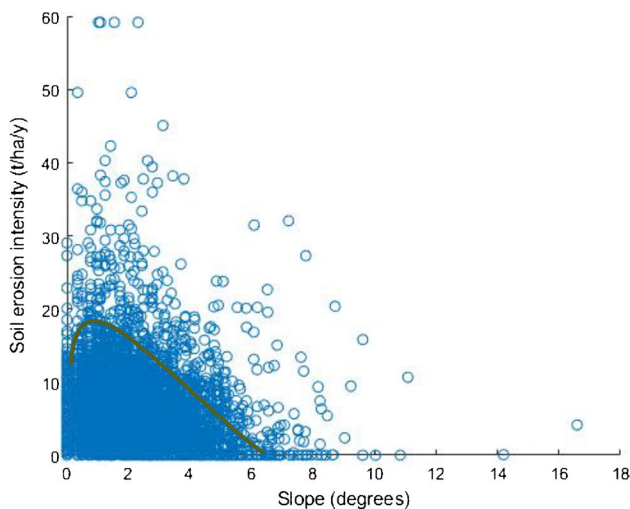
Fig. 9 Variation of soil erosion intensity (t/ha/year) with respect to slope of topography of the Kosi basin

Relation between average annual rainfall and soil erosion intensity

The relationship between average annual rainfall for the period 1985–2017, and soil erosion intensity has also been established with the same number of random samples and is shown in Fig. 10. It is observed from the figure that the soil erosion intensity increases with rainfall data in the selected time period.
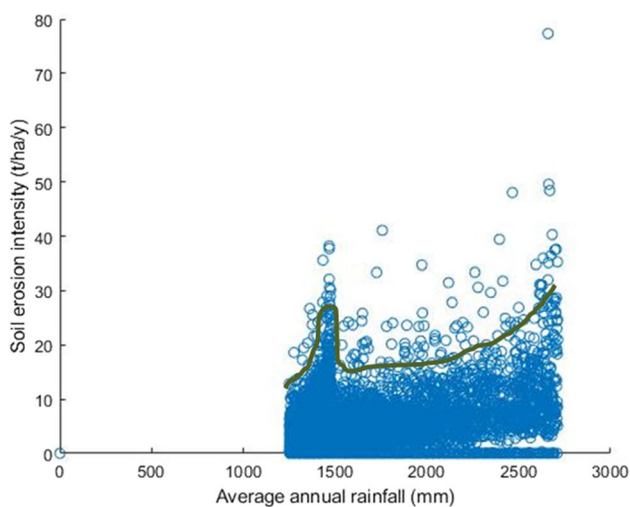

Fig. 10 Variation of soil erosion intensity (t/ha/year) with respect to the average annual rainfall (mm)

Discussions

Skilodimou et al. (2019) considered the factors such as precipitation, slope, land use, etc. for the application of the model for landslide susceptibility. Hence, the effect of these factors was seen in the change in soil erosion intensity from 2009 to 2019 in this study. From Fig. 3a and b, with reference to the soil erosion intensity (SEI), severe erosion was seen in the eastern portion of the Kosi river basin, which experienced a maximum rainfall during the selected time period. Percentage area of soil erosion was estimated and is grouped under five erosion intensities for seven subbasins. It was observed that subbasin 7 has the maximum slight erosion intensity for the years 2009 and 2019 near Kursela rain gauge station. The land use of subbasin 7 is mainly occupied with agricultural land as well as water bodies (Fig. 3). Besides these analyses, CI of soil erosion have also been estimated and found that majority of the selected area lies under stable zone. Maximum percentage of stable zone is found in subbasin 7; this may be due to higher percentage of agricultural land compared to other land cover classes (Figs. 3–5; Tables 4 and 5). Subbasins 3 and 5 were more affected due to intensive increase in soil erosion, and this may be due to the percentage increase in barren land and decrease in agricultural land as shown in Fig. 7. Subbasin 3 is mostly covered with barren land followed by forest (Fig. 3) which has slight erosion (54.54%), mild erosion (31.49%), moderate erosion (10.89%), and intensive erosion (2.72%) and severe erosion (0.36%) for the year 2009 and 44.72%, 32.92%, 15.98%, 5.43% and 0.89% respectively with change of $-9.82\%, +1.43\%, +5.09\%, +2.69\%$ and $+0.53\%$. These changes in soil erosion may be due to change in forest (-4%), barren land (4%) and agricultural (-4%) from 2009 to 2019 (Tables 4 and 5). Similarly, subbasin 5 has majority of agriculture and barren land and has 47.92% slight, 34.59% mild, 13.68% moderate, 3.45% intensive and 0.36% severe erosion in year 2009 and 41.20%, 33.25%, 18.05%, 6.32% and 1.18% in 2019 respectively with a change of $-6.72\%, +1.24\%, +4.37\%, +2.87\%$ and $+0.82\%$ respectively. These results are in accordance with the change in percentage of area in forest (-2%), barren land (3%) and agricultural (-4%) land.

The relationship of soil erosion with crop management factor (C) (Liu et al. 2020), slope of the terrain and average annual rainfall is vivid from the figures (Figs. 8–10). Figure 8a shows the skewed curve, and soil erosion intensity gets its peak in the early stage with reference to C factor as compared to the year 2019 (Fig. 8b). This skewness may be the most important factor with regard to the policy and the decisions of land use in which it represents conditions that can be most easily managed to reduce erosion. Slope parameter also plays a major role in the intensity of soil erosion (Guo et al. 2012). The soil erosion intensity increases for slope ranges from 0 to 1 degrees and then decreases. In other words, there is a positive relation between the

slope and the soil erosion up to the terrain slope of 1 degree, and it changes from positive to negative beyond this (Fig. 9). This variation of slope versus soil erosion intensity may reflect the greater soil loss due to heavy energy of runoff which is caused due to the greater gradient and length of slope (Jiang et al. 2014).

Based on the analysis of the change in soil erosion from 2009 to 2019 and the relationship between input parameters and soil erosion intensity, C factor plays a significant and effective role in the conservation of soil erosion in the Kosi river basin. As noted by Bathrellos et al. (2017), construction work and deforestation exacerbate soil erosion and the transportation of sediments and hence lead to degradation of land and flooding impact.

Conclusions

The Kosi river basin has a tendency of being affected by frequent floods and subsequent high sediment yield. Hence, the dynamic behaviour of soil erosions intensities has been evaluated under five slices from slight erosion intensity (< 1.50 t/ha/year) to severe erosion intensity (> 20.00 t/ha/year) for the years 2009 and 2019. In both the years, highest percentages of soil erosion were in the slight erosion intensity slice, i.e. 52.46% for 2009 and 45.39% for 2019. Least percentage areas of soil erosion are in severe erosion intensity slice in both the years. Apart from this, the whole Kosi basin has been delineated into seven subbasins with the help of SWAT tool and percentage areas of soil erosion for all the five slices were calculated. Subbasin 7 has the highest percentages of soil erosion in both years 2009 (74.91%) and 2019 (74.63%) for the slight erosion intensity. Change intensity (CI) in soil erosion between 2009 and 2019 was evaluated which ranges from intensive decrease (< -5.68 t/ha/year) to intensive increase (> 13.31 t/ha/year) and was found that 66.45% of the area is under stable range. Least percentage area lies in the intensive increase slice of change intensity and was found as 0.07%. The relationships have been established among annual soil erosion, crop management factor (C), percentage slope of the terrain and average annual rainfall. It was found that soil erosion gains its peak at the earlier stage in 2009 as compared to 2019, and the plot of 2009 is skewed towards its left, but the peak of soil erosion is found to be higher in the year 2019. The relation between percentage slope of the terrain and soil erosion intensity has also been established, and soil erosion is found to be increasing to an extent up to the percentage slope of one degree and then decreases. The dynamic behaviour of soil loss considering the C factor and terrain slope factor would help in the analysis of large basins like Kosi river basin carrying high sediment flux. This research gives an outlook on the relationships among various parameters used in soil erosion analysis. These observations are essential for further studies of subtropical belt, as the Kosi river basin is also located in the same subtropical belt.

Declarations

References

Al-Abadi AMA, Ghalib HB, Al-Qurnawi WS (2016) Estimation of soil erosion in northern Kirkuk governorate, Iraq using RUSLE, remote sensing and GIS. Carpathian J Earth Environ Sci 11(1):153–166

Anjali K, Roshni T (2021) Linking satellite-based forest cover change with rainfall and land surface temperature in Kerala, India. Environ Dev Sustain, 1-19. https://doi.org/10.1007/s10668-021-01908-w.

Ashiagbor G, Forkuo EK, Laari P, Aabeyir R (2013) Modeling soil erosion using RUSLE and GIS tools. Int J Remote Sens 2(4)

Bathrellos GD, Hariklia D, Konstantinos C, Ahmed MY, Biswajeet, (2017) Suitability estimation for urban development using multi-hazard assessment map. Sci Total Environ 575:119–134

Bhattacharyya R, Ghosh BN, Mishra PK, Mandal B, Rao CS, Sarkar D, Franzluebbers AJ (2015) Soil degradation in India: challenges and potential solutions. Sustain (switzerland) 7(4):3528–3570. https://doi.org/10.3390/su7043528

Boardman J (2006) Soil erosion science: reflections on the limitations of current approaches. CATENA 68(2–3):73–86. https://doi.org/10.1016/j.catena.2006.03.007

Borrelli P, Diodato N, Panagos P (2016) Rainfall erosivity in Italy: a national scale spatio-temporal assessment. Int J Digit Earth 9(9):835–850. https://doi.org/10.1080/17538947.2016.1148203

Estrada-carmona N, Harper EB, Declerck F, Fremier K (2017) Quantifying model uncertainty to improve watershed-level ecosystem service quantification : a global sensitivity analysis of the RUSLE. Int J Biodivers Sci Ecosyst Serv Manag 13(1):40–50. https://doi.org/10.1080/21513732.2016.1237383

Fayas CM, Abeysingha NS, Nirmanee KGS, Samaratunga D, Mallawatantri A (2019) Soil loss estimation using rusle model to prioritize erosion control in KELANI river basin in Sri Lanka. Int Soil Water Conserv Res 7(2):130–137. https://doi.org/10.1016/j.iswcr.2019.01.003

Ganasri BP, Ramesh H (2016) Assessment of soil erosion by RUSLE model using remote sensing and GIS - A case study of Nethravathi Basin. Geosci Front 7(6):953–961. https://doi.org/10.1016/j.gsf.2015.10.007

Guo B, Tao HP, Liu BT, Jiang L (2012) Characteristics and analysis of soil erosion in Li country after Wenchuan earthquake based on GIS and USLE. Trans Chin Soc Agric Eng 28:118–126. https://doi.org/10.3969/j.issn.1002-6819.2012.14.019

Gupta S, Kumar S (2017) Simulating climate change impact on soil erosion using RUSLE model − a case study in a watershed of mid-Himalayan landscape. J Earth Syst Sci 126(3). https://doi.org/10.1007/s12040-017-0823-1

Himayoun D, Roshni T (2020) Geomorphic changes in the Jhelum River due to an extreme flood event: a case study. Arab J Geosci 13(2):1–5

Jemai S, Kallel A, Agoubi B, Abida H (2021) Soil erosion estimation in arid area by USLE Model applying GIS and RS: case of Oued El Hamma Catchment, South-Eastern Tunisia. J Indian Soc Remote Sens 49(6):1293–1305. https://doi.org/10.1007/s12524-021-01320-x

Jiang L, Bian JH, Li AN, Lei GB, Nan X, Feng WL, Li G (2014) Spatial-temporal changes of soil erosion in the upper reaches of Minjiang River from 2000 to 2010. J Soil Water Conserv 28:19–25. https://doi.org/10.3969/j.issn.1009-2242.2014.01.004

Kayet N, Pathak K, Chakrabarty A, Sahoo S (2018) Evaluation of soil loss estimation using the RUSLE model and SCS-CN method in hillslope mining areas. Int Soil Water Conserv Res 6(1):31–42. https://doi.org/10.1016/j.iswcr.2017.11.002

Kim HS (2006) Soil Erosion Modeling Using RUSLE and GIS on the IMHA Watershed, South Korea. Doctoral dissertation. Colorado State University, USA. https://www.koreascience.or.kr/article/JAKO200606140780380.page

Kumar R, Jain V, Prasad Babu G, Sinha R (2014) Connectivity structure of the Kosi megafan and role of rail-road transport network. Geomorphology 227:73–86. https://doi.org/10.1016/j.geomorph.2014.04.031

Kumar S, Roshni T (2019) NDVI-rainfall correlation and irrigation water requirement of different crops in the Sone river-command. Bihar MAUSAM 70(2):339–346

Kumar S, Roshni T, Kahya E, Ghorbani MA (2020) Climate change projections of rainfall and its impact on the cropland suitability for rice and wheat crops in the Sone river command. Bihar Theor Appl Climatol 142(1–2):433–451. https://doi.org/10.1007/s00704-020-03319-9

Lal R (2001) Soil degradation by erosion. Land Degrad Dev 12:519–539. https://doi.org/10.1002/ldr.472

Li Z, Liu C, Dong Y, Chang X, Nie X, Liu L, Zeng G (2017) Response of soil organic carbon and nitrogen stocks to soil erosion and land use types in the Loess hilly–gully region of China. Soil Tillage Res 166:1–9. https://doi.org/10.1016/j.still.2016.10.004

Liu Y, Zhao W, Liu Y, Pereira P (2020) Global rainfall erosivity changes between 1980 and 2017 based on an erosivity model using daily precipitation data. CATENA 194:104768. https://doi.org/10.1016/j.catena.2020.104768

Mishra K, Sinha R (2020) Geomorphology Flood risk assessment in the Kosi megafan using multi-criteria decision analysis : a hydrogeomorphic approach. Geomorphology 350:106861. https://doi.org/10.1016/j.geomorph.2019.106861

Morgan RPC (2005) Soil erosion & conservation. Blackwell, Australia

Naipal V, Reick C, Pongratz J, Van Oost K (2015) Improving the global applicability of the RUSLE model - adjustment of the topographical and rainfall erosivity factors. Geosci Model Dev 8(9):2893–2913. https://doi.org/10.5194/gmd-8-2893-2015

Narayana BDVV (1984) Estimation of soil erosion in India. 109(4):419–434

Nearing MA, Foster GR, Lane LJ, Finckner SC (1989) A process-based soil erosion model for USDA- Water Erosion Prediction Project technology. Trans Am Soc Agric Eng 32:1587–1593

Panagos P, Ballabio C, Borrelli P, Meusburger K, Klik A, Rousseva S, Alewell C (2015) Rainfall erosivity in Europe. Sci Total Environ 511:801–814. https://doi.org/10.1016/j.scitotenv.2015.01.008

Rajbanshi J, Bhattacharya S (2020) Assessment of soil erosion, sediment yield and basin specific controlling factors using RUSLE-SDR and PLSR approach in Konar river basin. India J Hydrol 587(January):124935. https://doi.org/10.1016/j.jhydrol.2020.124935

Renard KG, Freimund JR (1994) Using monthly precipitation data to estimate the R-factor in the revised USLE. J Hydrol 157(1–4):287–306

Renard K, Foster G, Weesies G, McCool D, Yoder D (1997) Predicting Soil erosion by water: A Guide to Conservation Planning with the Revised Universal Soil Loss Equation (RUSLE). US Department

of Agriculture, Agriculture Handbook No.703USDA, USDA, Washington DC

Reusing M, Schneider T, Ammer U (2000) Modelling soil loss rates in the Ethiopian Highlands by integration of high resolution MOMS-02/D2-stereo-data in a GIS. Int J Remote Sens 21(9):1885–1896. https://doi.org/10.1080/014311600209797

Robinson DA, Panagos P, Borrelli P, Jones A, Montanarella L, Tye A, Obst CG (2017) Soil natural capital in Europe; a framework for state and change assessment. Sci Rep 7(1):1–14. https://doi.org/10.1038/s41598-017-06819-3

Rozos D, Skilodimou HD, Loupasakis C, Bathrellos GD (2013) Application of the revised universal soil loss equation model on landslide prevention. An example from N. Euboea (Evia) Island. Greece Environ Earth Sci 70:3255–3266

Sinha R, Gupta A, Mishra K, Tripathi S, Nepal S, Wahid SM (2018) Swarnkar S (2019) Basin-scale hydrology and sediment dynamics of the Kosi river in the Himalayan foreland. J Hydrol 570:156–166. https://doi.org/10.1016/j.jhydrol.2018.12.051

Skilodimou HD, Bathrellos GD, Chousianitis K, Youssef AM, Pradhan B (2019) Multi-hazard assessment modeling via multi-criteria analysis and GIS: a case study. Environ Earth Sci 78(2):1–21. https://doi.org/10.1007/s12665-018-8003-4

Towheed A, Roshni T (2021) Linking climate change to soil loss estimation in the Kosi river basin, India. J Water Clim Change 1–26. https://doi.org/10.2166/wcc.2021.259

Uddin K, Murthy MSR, Wahid SM, Matin MA (2016) Estimation of soil erosion dynamics in the Koshi basin using GIS and remote sensing to assess priority areas for conservation. PLoS One 11(3). https://doi.org/10.1371/journal.pone.0150494

Vijith H, Suma M, Rekha VB, Shiju C, Rejith PG (2012) An assessment of soil erosion probability and erosion rate in a tropical mountainous watershed using remote sensing and GIS. Arab J Geosci 5(4):797–805. https://doi.org/10.1007/s12517-010-0265-4

Wischmeier WH, Smith DD (1978) Predicting rainfall erosion losses: A Guide to Conservation Planning. The USDA Agricultural Handbook No. 537, Maryland

Xu Y, Shao X, Kong X, Peng J, Cai Y (2008) Adapting the RUSLE and GIS to model soil erosion risk in a mountains karst watershed, Guizhou Province, China, pp 275–286

Xu L, Xu X, Meng X (2013) Risk assessment of soil erosion in different rainfall scenarios by RUSLE model coupled with information diffusion model: a case study of Bohai Rim, China. CATENA 100:74–82. https://doi.org/10.1016/j.catena.2012.08.012

Yang D, Kanae S, Oki T, Koike T, Musiake K (2003) Global potential soil erosion with reference to land use and climate changes. Hydrol Process 17(14):2913–2928. https://doi.org/10.1002/hyp.1441

Yue-qing X, Xiao-mei S, Xiang-bin K (2008) Adapting the RUSLE and GIS to model soil erosion risk in a mountains karst watershed , Guizhou Province , China. Environ Monit Assess, 275–286. https://doi.org/10.1007/s10661-007-9894-9

Zhou P, Luukkanen O, Tokola T, Nieminen J (2008) Catena Effect of vegetation cover on soil erosion in a mountainous watershed. CATENA 75(3):319–325. https://doi.org/10.1016/j.catena.2008.07.010

Zhu X, Zhang R, Sun X (2021) Spatiotemporal dynamics of soil erosion in the ecotone between the Loess Platau and Western Qinling Mountains based on RUSLE modeling, GIS, and remote sensing. Arab J Geosci 14(1). https://doi.org/10.1007/s12517-020-06329-z